Influence of Stacking Interactions on NMR Chemical Shielding Tensors in Benzene and Formamide Homodimers as Studied by HF, DFT and MP2 Calculations

Jiří Czernek*

Institute of Macromolecular Chemistry, Academy of Sciences of the Czech Republic, Heyrovsky Sq. 2, 162 06 Praha 6, The Czech Republic

Received: November 21, 2002; In Final Form: February 11, 2003

A systematic investigation of the dependencies of the isotropic chemical shielding and the chemical shielding anisotropy upon the vertical-stacking distance for the respective ^{15}N, ^{1}H, and ^{13}C nuclei present in simple models representing the aromatic and nonaromatic stacking (i.e., in benzene and formamide dimers accordingly) has been carried out. Although the approaches employed differ in the way they treat the effects of electron correlation and hence their ability to account for the energetics of stacking varies significantly, the qualitative characteristics of the stacking-induced variation in the chemical shielding parameters remain unchanged. This substantiates the use of the computationally cheap, DFT-based methods (the SOS-DFPT-IGLO strategy in particular) in modeling the secondary structural effects on chemical shielding parameters of biomolecular systems.

Introduction

Noncovalent interactions affect many fundamental chemical, physical, and biochemical processes and are a topical area of both experimental and theoretical research.[1] One of the major manifestations of noncovalent forces are stacking interactions. They influence the three-dimensional structure of biological macromolecules such as proteins[2] and nucleic acids,[3] confer stability and specificity in RNA−ligand complexes,[4] define binding of intercalators to DNA,[5] etc. Remarkable progress has been achieved in the quantitative description of the energetics of stacking in model systems (see refs 6 and 7 and references therein). Using high level ab initio methods and ample basis sets, currently, it is becoming possible to obtain precise stacking energies.[8] Thus, a quantum chemical description of energetic surfaces of suitably chosen models can usefully supplement experimental studies of, for example, thermodynamics of stacking.[9] Moreover, it also provides for reliable reference data used in developing more accurate empirical potentials for subsequent use in classical molecular dynamics and Monte Carlo simulations of large (bio)molecular systems.

NMR measurements have developed into an important tool to probe stacking interactions. Examples range from numerous studies on self-stacking of organic compounds using temperature-dependent 1D ^{1}H NMR measurements,[10] through the most recent evidence, obtained employing the ^{19}F, ^{1}H−HOESY technique, for inorganic acid−base stacking in solution,[11] to ^{15}N and ^{13}C NMR investigations of complex biomolecular systems in which global structural information is incomplete.[12] However, theoretical understanding of the influence of stacking interactions upon chemical shielding tensors is rather limited. In the case of aromatic stacking (i.e., for the attraction between π systems), ring-current theories have been usually invoked (see ref 13 for review). When properly adjusted, ring-current models can provide some insight into stacking contributions to chemical shifts[14] and even chemical shielding anisotropies.[15] Nevertheless, they are not directly applicable to an analysis of the full tensorial information, i.e., to principal elements of the chemical shielding tensor and their orientation in the reference axis system.[16] Instead, high-level quantum chemical methods of chemical shielding calculations (recently reviewed in ref 17) can currently be applied to the stacked complexes. Examples published so far include scouting computations by Cui and Karplus[18] and by Xu et al.[19] of practically important stacking between nucleic acid bases (density functional theory (DFT)[20]-based methodologies have been used). Moreover, Gauss et al. performed extensive ^{1}H chemical shielding tensor calculations at the Hartree−Fock (HF) level for hexabenzocoronene derivatives to facilitate solid-state NMR studies of the molecular arrangements in condensed phases.[21] Apparently, no ab initio calculations of chemical shielding tensors have been presented for systems exhibiting the nonaromatic stacking.[22]

In this report, the chemical shielding tensors of several nuclei in benzene and formamide homodimers, i.e., in systems representing simple models of $\pi-\pi$ and nonaromatic stacking, respectively, have been carefully investigated. Results for similar systems (formamidine and pyrimidine homodimers) are also given. HF, DFT, and MP2 (second-order Møller−Plesset perturbation theory) techniques and several basis sets have been employed. In particular, the trends in changes with the distance between stacked monomers of the isotropic chemical shieldings and the chemical shielding anisotropies have been established for the first time. Significantly, we demonstrate that despite the well-known failure of the HF and DFT methods to correctly describe the interaction potential for the systems investigated the variation in chemical shielding data can be recovered using approaches that are by far less demanding than MP2. This is important not only from the theoretical perspective but also practically. For example, for systems with a significant dispersion energy component, i.e., the stacked complexes of benzene with methane[23] and benzene with *N*-methyl acetamide,[15] various DFT techniques have been previously adopted to account for the ring-current effects on NMR parameters. A DFT-based method is also being employed in an extensive investigation of

* To whom correspondence should be addressed. Fax: +420-296809410. Phone: +420-296809290. E-mail: czernek@imc.cas.cz.

10.1021/jp022467x CCC: $25.00
Published on Web 04/15/2003

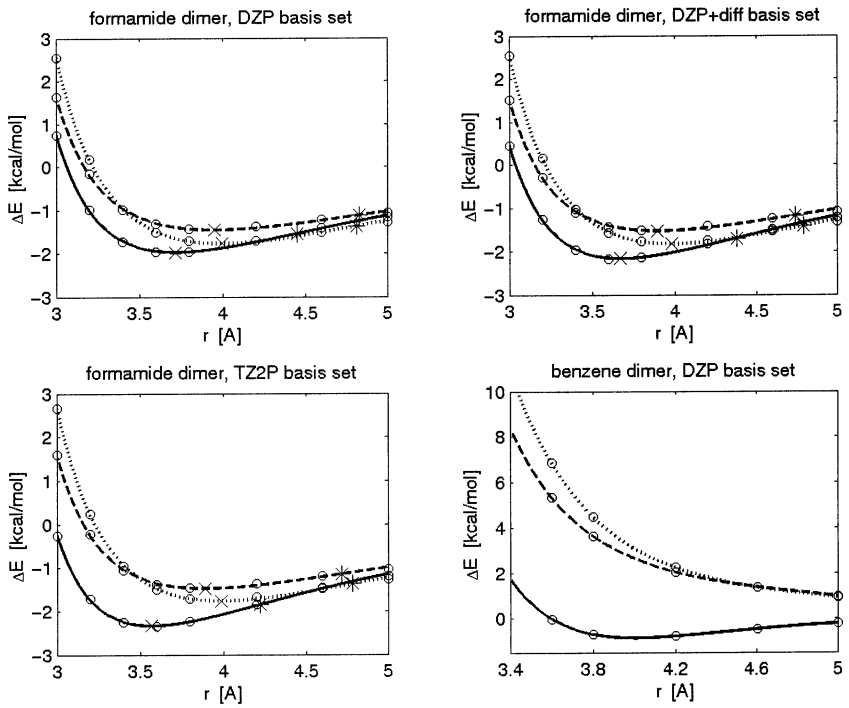

Figure 1. Potential energy curves of stacking. MP2, B3LYP, and HF curves are represented by solid, dashed, and dotted lines, respectively. For the formamide dimer, they have been obtained according to eq 5, and the cubic spline interpolation has been used in the case of the benzene dimer. The computed points, minima, and inflex points are marked as circles, crosses, and asterisks, respectively. See the text for details.

the influence of stacking upon the ^{1}H and ^{15}N chemical shifts in fragments of nucleic acids.[24] The present study indicates that computationally less expensive approaches can be used to reliably describe the contribution of stacking to the variation in the chemical shielding tensors, and thus, they can furnish results directly applicable in, for example, liquid- and solid-state NMR studies of biological macromolecules.

Methods

As for the benzene dimer (BD), the parallel arrangement of two benzene molecules has been investigated in the MP2/6-31G* geometry taken from ref 6 (D_{6h} symmetry; the structure referred to as dimer A by the authors). The coordinates of the formamide dimer (FD) have been prepared by optimizing the planar monomer at the MP2/6-31G* level and creating the antiparallel structure (ref 22, Figure 1a) possessing C_i symmetry. For both BD and FD, the calculations of energies and chemical shielding tensors have been carried out at the vertical separation between constituting monomers, *r*, of 3.0, 3.2, 3.4, 3.6, 3.8, 4.2, 4.6, and 5.0 Å. This interval lies within the range of distances between stacked organic molecules in the crystalline state (cf. an extensive survey by Dahl[25]). Scouting calculations for base pairs of nucleic acids (J. Czernek, unpublished results) have suggested that the dependence of chemical shielding tensors upon the changes of buckle, propeller, opening, and twist is relatively minor when compared to the influence exerted by modifying the vertical intermonomer separation.

Compared to the HF and, especially, DFT treatments, memory and disk requirements of MP2 chemical shielding calculations grow very fast with the number of basis functions. Consequently, it is of interest to compare results obtained using several basis sets of increasing size and quality to be able to assess the basis set dependence of the trends in chemical shielding changes. Thus, the smallest basis set considered is the polarized double-ξ (DZP).[2627,28] Its contraction pattern is (4;1)/[3,1;1] for hydrogen and (9;5;1)/[6,3*1;4,1;1] for first row atoms. As it has been repeatedly exemplified that diffuse functions are important for the proper description of the energetics of stacking,[29] the polarized double-ξ basis set augmented with one set of diffuse functions (DZP+diff) by Dunning and Hay[26−28] was examined as well. It contains one s-type diffuse function on hydrogens and one p-type diffuse function on the remaining first-row atoms. The DZP+diff basis set has been selected because it was recently shown to reliably describe the dimethylformamide dimers.[30] The third basis set employed is the triple-ξ basis set with two sets of polarization functions (TZ2P) by Schäfer et al.[31] Its contraction pattern is (5;2)/[3,2*1;1,1] for hydrogens and (10;6;2)/[5,5*1;4,2*1;1,1] for the remaining atoms. The values of polarization exponents are 0.39 and 1.39 for H, 0.44 and 1.58 for C, 0.58 and 1.73 for N, and 0.69 and 2.08 for O. MP2 chemical shielding calculations with the above-mentioned basis sets have only been carried out for the formamide dimer (120, 144, and 204 basis functions for DZP, DZP+diff, and TZ2P, respectively). The benzene dimer has been investigated employing the DZP basis set (240 basis functions) and also using TZ2P (404 basis functions, HF and B3LYP calculations only). Moreover, the SOS-DFPT-IGLO chemical shielding computations (vide infra) have been performed using the IGLO-III basis set of Kutzelnigg et al.[32] and with a huge JMN2 basis set.[33] IGLO-III is of roughly quadruple-ξ quality with two sets of polarization functions (the contraction pattern (6;2)/[3,3*1;1,1] for H and (11;7;2)/[5,6*1;2,5*1;1,1] for (C,N,O)). The JMN2 is the uncontracted IGLO-III basis set with two additional sets of polarization functions. The use of the IGLO-III resulted in application of 282 and 564 basis functions for FD and BD accordingly. In the case of the JMN2 basis set, the number of basis functions was 444 and 888, respectively.

The chemical shielding tensors at the HF and MP2[34] levels have been calculated with the gauge-including atomic orbital (GIAO) formalism[35,36] using the Gaussian 98 suite of programs.[37] The GIAO method of overcoming the gauge problem was also combined with the B3LYP (Becke's three parameter

exchange[38] and Lee, Yang, Parr correlation[39]) DFT functional. In this scheme, the coupled-perturbed Kohn−Sham equations with the presence of Hartree−Fock exchange terms are solved; the implementation in Gaussian 98 has been used.[40] SOS-DFPT-IGLO shielding tensors have been obtained with the deMon-MASTER−CS code[41,42] which implements sum-over-stated density functional (Rayleigh−Schrödinger) perturbation theory with the individual gauges for localized orbitals (IGLO).[32] The Perdew-Wang-91 exchange-correlation potential,[43,44] the FINE angular integration grid with 64 radial shells,[33] and the approximation Loc. 1 SOS-DFPT[45] have been used. The molecular orbitals have been localized by the method of Boys.[46] In what follows, the resulting approaches for chemical shielding calculations will be denoted simply as HF, MP2, B3LYP, and SOS-DFPT.

Principal components of the chemical shielding tensor of selected atoms (see Results and Discussion) as provided by the above-mentioned programs, $\sigma_{11} \leq \sigma_{22} \leq \sigma_{33}$, have been used to calculate the isotropic chemical shielding, σ^{iso}

$$\sigma^{iso} = 1/3(\sigma_{11} + \sigma_{22} + \sigma_{33}) \quad (1)$$

and the part of the chemical shielding anisotropy responsible for autocorrelation processes, CSA_a

$$CSA_a = \sqrt{{\sigma_{11}}^2 + {\sigma_{22}}^2 + {\sigma_{33}}^2 - \sigma_{11}\sigma_{22} - \sigma_{11}\sigma_{33} - \sigma_{22}\sigma_{33}} \quad (2)$$

The parameter CSA_a has been chosen for the presentation of the changes in chemical shielding anisotropy, because simplified assumptions about axial symmetry of the chemical shielding tensor are not invoked in its definition. See references 47 and 48 for a thorough discussion of different definitions of chemical shielding anisotropies.

McConnell equation[49] has been used to model the change, which is brought about by the presence of stacking benzene molecule, in the isotropic chemical shift of a proton in benzene, $\Delta\delta$. In the present case, based on symmetry considerations, let $\vec{R}$ denotes the vector pointing from the proton in one benzene molecule to the center of symmetry of the second benzene, R is the Euclidean length of $\vec{R}$, θ is the angle between $\vec{R}$ and the χ_{11} principal component of the molecular magnetic susceptibility (magnetizability) tensor of benzene (χ_{11} is perpendicular to the benzene ring), and χ^{aniso} is the anisotropy of the molecular magnetic susceptibility tensor of benzene ($\chi^{aniso} = \chi_{11} - 1/2(\chi_{22} + \chi_{33})$, where χ_{22} and χ_{33} are the in-plane principal components). McConnell equation thus takes the form

$$\Delta\delta = \frac{1}{3R^3}\chi^{aniso}(3\cos^2\theta - 1) \quad (3)$$

which can be easily rearranged into

$$\Delta\delta = \chi^{aniso}\frac{2r^2 - d^2}{3(d^2 + r^2)^{5/2}} \quad (4)$$

where d is the distance from the center of symmetry of benzene to the proton ($d = 2.4824$ Å at the MP2/6-31G* level) and r is the vertical separation between the monomers. Note that the functional form expressed by eq 4 explicitly relates $\Delta\delta$ to the separation between benzene molecules. The molecular magnetic susceptibility tensor of benzene has been calculated using the CSGT method[50] as implemented in the Gaussian 98 program package. In this approach, gauge-invariance is achieved by performing a continuous set of gauge transformations, and the magnetic susceptibility (and chemical shielding) tensor is determined from the current density (see refs 51 and 52 for details). For a more consistent comparison of $\Delta\delta$'s predicted by the McConnell equation with their quantum chemical counterparts, the chemical shielding tensors of the benzene dimer have also been obtained with the CSGT gauge choice using the implementation in the Gaussian 98.[40] The B3LYP/TZ2P DFT approach has been adopted with the CSGT calculations.

The interaction energies, ΔE, have been obtained using the variational supermolecular approach; the basis set superposition error (BSSE) was corrected for by means of the counterpoise method.[53] For the formamide dimer, the potential energy curves of stacking, i.e., the dependencies of ΔE on r, have been fitted in the least-squares sense to the form

$$\Delta E(r;C_6,C_7,C_8,C_9) = C_6 r^{-6} + C_7 r^{-7} + C_8 r^{-8} + C_9 r^{-9} \quad (5)$$

An inclusion of the $C_n r^{-n}$ terms from $n = 6$ up to $n = 9$ has been found necessary to ensure the correlation coefficient R^2 values are higher than 0.999, and the variances of residuals, σ^2, are smaller than 0.0016. Subsequently, the positions of a minimum, r_{min}, and of an inflex point, r_{inflex}, of the potential energy curves have been calculated by computing

$$\frac{d\Delta E(r;C_6,C_7,C_8,C_9)}{dr}$$

and

$$\frac{d^2\Delta E(r;C_6,C_7,C_8,C_9)}{dr^2}$$

respectively, and solving these expressions for 0.

Results and Discussion

Energetics. The HF, B3LYP, and MP2 interaction energies and BSSE values computed with the DZP, DZP+diff, and TZ2P basis sets (for the formamide dimer) and the DZP basis set (the benzene dimer) are available as Supporting Information (Tables 1S−4S). Estimated r_{min} and r_{inflex}data (see above) together with respective $\Delta E(r_{min})$ and $\Delta E(r_{inflex})$values are also given with Tables 1S−3S. The statistical data concerning eq 5 and the total energies of all structures can be obtained from the author upon request. The potential energy curves are shown in Figure 1. It should be mentioned that several high-level theoretical investigations of the binding energy of the benzene dimer exist,[54] and the formamide dimer has been studied in detail at the CCSD(T) level.[55] Hence, the present results serve exclusively as a demonstration of qualitative differences between ΔE's as provided by respective methods and do not aim in obtaining data of supreme accuracy.

It has been repeatedly stressed in the literature that both the Hartree−Fock method and current approximate exchange-correlation functionals within the Kohn−Sham framework are unable to correctly account for the dispersive interactions and thus are not expected to provide accurate interaction energies of weakly bound complexes (including stacked ones).[56] For example, it has been recognized for a long time that HF and DFT methods fail completely to describe the attraction in the benzene dimer: a repulsive interaction is predicted (see Figure 1, the subplot on the right of the second row). In the case of nonaromatic stacking, our MP2/TZ2P values agree within 0.2 kcal/mol with the results of the MP2/aug-cc-pVDZ step by step optimization of the vertical separation of the stacked formamide monomers published by Hobza and Šponer (Table 2 of Ref 55).

TABLE 1: Amidic ^{15}N Isotropic Chemical Shielding (ppm) and Chemical Shielding Anisotropy (in Parentheses, ppm) at Different Vertical Separations between Formamide Monomers (r, Å) as Predicted by Various Approaches[a]

	DZP			DZP+			TZ2P			
r	MP2	HF	B3LYP	MP2	HF	B3LYP	MP2	HF	B3LYP	SOS-DFPT
3.0	170.1	158.5	140.0	168.2	156.8	138.2	153.7	145.8	126.8	127.7
	(138.7)	(159.6)	(154.3)	(146.1)	(163.1)	(159.6)	(157.8)	(171.0)	(168.0)	(160.6)
3.2	174.4	162.8	144.7	172.6	161.8	142.9	158.2	150.2	130.9	132.2
	(140.9)	(161.0)	(156.2)	(149.0)	(165.3)	(162.0)	(161.1)	(173.3)	(170.8)	(163.3)
3.4	177.1	165.6	147.7	175.5	164.7	146.0	161.2	153.0	134.7	135.1
	(142.2)	(161.7)	(157.2)	(150.8)	(166.4)	(163.3)	(163.1)	(174.6)	(173.2)	(164.9)
3.6	178.9	167.3	149.7	177.3	166.5	148.1	163.1	154.8	136.8	136.9
	(142.8)	(161.9)	(157.7)	(151.7)	(167.0)	(164.1)	(164.3)	(175.3)	(174.3)	(165.9)
3.8	180.0	168.5	150.9	178.5	167.6	149.4	164.3	156.0	138.1	138.2
	(143.1)	(161.9)	(157.9)	(152.1)	(167.3)	(164.4)	(164.9)	(175.7)	(174.9)	(166.4)
4.2	181.2	169.6	152.2	179.7	168.9	150.9	165.6	157.4	139.7	139.3
	(143.1)	(161.6)	(157.8)	(152.1)	(167.3)	(164.4)	(165.3)	(175.7)	(175.1)	(166.1)
4.6	181.7	170.1	152.7	180.3	169.5	151.6	166.4	158.1	140.6	140.0
	(142.9)	(161.3)	(157.5)	(151.7)	(167.0)	(164.0)	(165.1)	(175.4)	(174.9)	(165.7)
5.0	181.9	170.4	153.0	180.7	169.9	152.1	166.8	158.5	141.1	140.3
	(142.7)	(160.9)	(157.3)	(151.2)	(166.5)	(163.5)	(164.9)	(175.0)	(174.7)	(165.3)

[a] See the text for the description of respective computational methods.

Consequently, the former data will be used to benchmark the results of the remaining approaches adopted here. As it might be anticipated, both the HF and B3LYP methods provide too crude a description of the potential energy curves of stacking. Specifically, these methods tend to underestimate the well depths and provide far too long equilibrium intemonomer separations and rather flat potential energy curves (see the corresponding subplots of Figure 1). For example, in the case of the TZ2P basis set, the HF and B3LYP $\Delta E(r_{min})$ values are −1.76 and −1.48 kcal/mol, respectively, as compared to the MP2 value of −2.34 kcal/mol; the HF and B3LYP r_{min}'s lie at approximately 3.99 and 3.89 Å, respectively, whereas their MP2 counterpart is located at 3.57 Å; the HF and B3LYP r_{inflex} values (4.78 and 4.72 Å accordingly) are separated by ca. 0.5 Å from the MP2 r_{inflex}= 4.22 Å. Such an inadequate behavior of the HF and DFT methods in the description of the energetics of nonaromatic stacking is also apparent for computations using smaller basis sets. Interestingly, the MP2 potential energy curves of stacking benefited more from the extension of the basis set from DZP to TZ2P than from the augmentation of the DZP with diffuse functions. Refer to Figure 1 and Supporting Information Tables 1S−3S for further details.

Formamide Dimer. Now we will turn to the description of the chemical shielding property. We start with the ^{15}N chemical shielding of the amidic nitrogen(s) in the formamide dimer. The values of the σ^{iso}(N) and CSA_a(N) computed at respective intermonomer separations are summarized in Table 1, and Figure 2 graphically illustrates the σ^{iso}(N) data (the TZ2P basis set has been used with the GIAO-based approaches).

A full account of the tensor components as computed by HF, MP2, B3LYP, and SOS-DFPT methods using several basis sets is given in Supplementary Information (Tables 5S−8S). For all methods and basis sets considered, a monotonic increase of the σ^{iso}(N) with the distance between monomers can be seen. The overall change is significant: the predicted differences between the σ^{iso}(N) at r = 3.0 and 5.0 Å range from −11.8 (MP2/DZP) to −14.3 ppm (B3LYP/TZ2P). The influence of the basis set on computed σ^{iso}(N) values is apparent from Figures 3 and 4, where the DZP, DZP+diff, and TZ2P data are shown for the MP2 and HF calculations accordingly. Clearly, the bigger the basis set, the less shielded the amidic nitrogen becomes. The deshielding with respect to the DZP results is much more pronounced for the TZ2P than DZP+diff data. As for the basis set dependence of the SOS-DFPT-IGLO calculations, the maximum differences between the results obtained with the IGLO-III and JMN2 basis sets are 1.6 ppm for the principal components of the σ(N) and only 0.36 ppm for the isotropic chemical shielding of the amidic nitrogen.

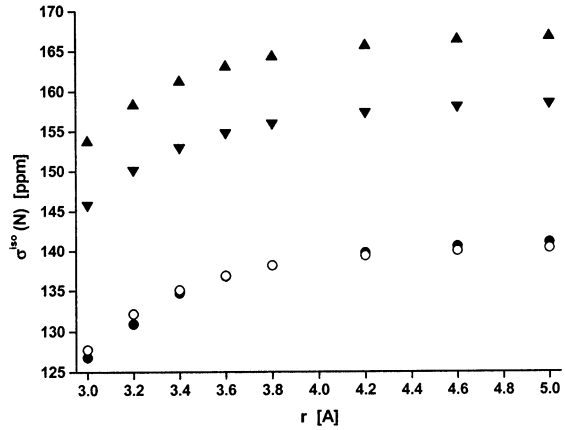

Figure 2. Plot of the ^{15}N isotropic chemical shielding of amidic nitrogen in the formamide dimer σ^{iso}(N) computed at different vertical separations between monomers r by the MP2 (up triangles), HF (down triangles), B3LYP (solid circles), and SOS-DFPT (open circles) methods. See the text for details.

It is noted that for all combinations of methods and basis sets the increase of the σ^{iso}(N) with the distance r can be accurately fitted to the form

$$\sigma^{iso}(N) = \frac{a}{1 + \exp(br)} + c \qquad (6)$$

containing only three parameters, i.e., a, b, and c (not shown).

It is not unexpected the HF and DFT σ^{iso}(N) values are uniformly too deshielded with respect to the MP2 data; this effect appears to be caused mostly by deficiencies in the description of the virtual Hartree−Fock and Kohn−Sham orbitals (see ref 57 for the most recent development and references concerning this problem). Remarkably however, the deshielding, while as large as 30 ppm when smaller basis sets are employed, remains fairly constant in the whole range of vertical separations investigated. For example, the |MP2 − HF| and |MP2 − B3LYP| data obtained with the TZ2P basis set lie between 7.88 and 8.28 ppm (mean value 8.18 ppm, standard deviation 0.138 ppm), and 25.71 and 27.33 ppm (mean value 26.32 ppm, standard deviation 0.565 ppm), respectively. It is worth remarking that |MP2 − HF| differences are commonly

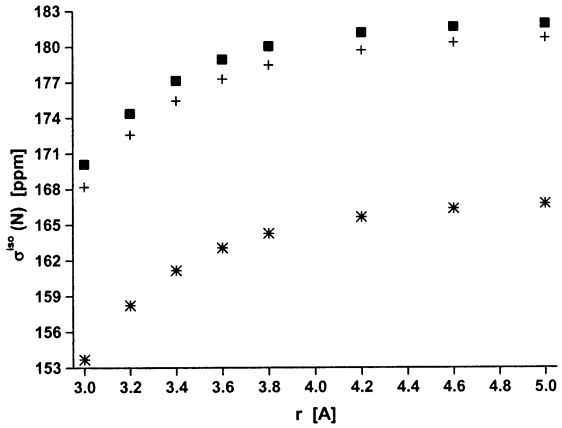

Figure 3. Plot of the ^{15}N isotropic chemical shielding of amidic nitrogen in the formamide dimer σ^{iso}(N) computed at different vertical separations between monomers r by the MP2-GIAO method with the DZP (squares), DZP+diff (crosses), and TZ2P (stars) basis sets.

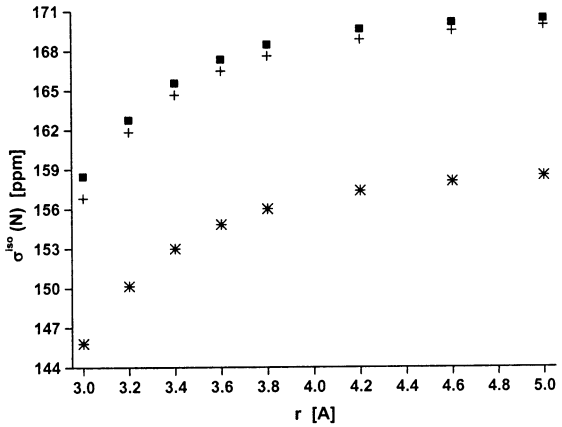

Figure 4. Plot of the ^{15}N isotropic chemical shielding of amidic nitrogen in the formamide dimer σ^{iso}(N) computed at different vertical separations between monomers r by the HF-GIAO method with the DZP (squares), DZP+diff (crosses), and TZ2P (stars) basis sets.

considered as an upper bound of the electron correlation contributions to chemical shielding[58] (see also references 17 and 59). This suggests that the correlation effects on the σ^{iso}(N) remain practically constant, at least within the studied interval.

The dependence of the CSA_a of amidic nitrogen on r is less dramatic than in the case of the absolute isotropic shielding (see Table 1). After an initial increase in the CSA_a(N) values of up to 8 ppm in the interval between 3.0 and about 4 Å, the results are predicted to mildly decrease when r approaches 5.0 Å. This behavior is common to all methods and basis sets investigated here and is exemplified in Figure 5 (the TZ2P basis set has been used with the GIAO-based approaches). It is noteworthy that the fastest approach employed, i.e., SOS-DFPT/IGLO-III (see refs 47, 48, and 60 for details), fortuitously provides the CSA_a(N) values very similar to the MP2/TZ2P data.

As there is an eminent interest in understanding, using simple models of biomolecules, of various structural contributions to the H^N proton chemical shielding in proteins,[61] we will briefly discuss the results obtained for the amidic proton(s) in the formamide dimer as well. The changes of the σ^{iso}(H) and CSA_a(H) with the vertical separation between monomers are collected in Table 2. The complete set of the σ_{ii}(H)'s is given as Supplementary Information Tables 9S−12S.

The isotropic chemical shielding of the amidic proton is predicted to be virtually unaffected by the nonaromatic stacking. This facet can be traced back to an almost-perfect cancellation

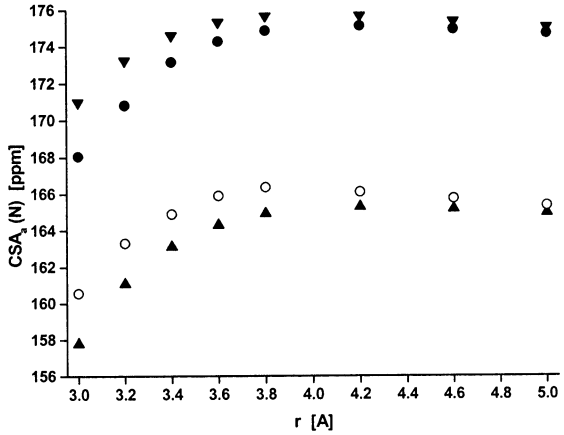

Figure 5. Plot of the ^{15}N chemical shielding anisotropy of amidic nitrogen in the formamide dimer CSA_a(N) computed at different vertical separations between monomers r by the MP2 (up triangles), HF (down triangles), B3LYP (solid circles), and SOS-DFPT (open circles) methods. See the text for details.

of changes in respective principal values with increasing r (cf. eq 1): while σ_{11} diminishes with increasing the intermonomer separation, the remaining two tensor components increase (see Tables 9S−12S). On the other hand, the CSA_a(H) values grow roughly 1 ppm when going from $r = 3.0$ to 5.0 Å. This increase can be simply and accurately approximated with the second order polynomial (data not shown). As was the case with the chemical shielding data of the amidic nitrogen, all methods and basis sets employed qualitatively agree in the trends predicted for the changes in σ^{iso}(H) and CSA_a(H). The maximum difference between data obtained by the SOS-DFPT method using the IGLO-III and JMN2 basis sets is 0.31 ppm for the σ_{ii}(H) and only 0.13 ppm for the σ^{iso}(H).

Benzene Dimer. Let us now describe the influence of stacking upon the ^{13}C and ^{1}H chemical shielding tensors in the sandwich configuration of the benzene dimer. The principal components as provided by various approaches are detailed in Supporting Information Tables 13S−19S. Before discussing respective tendencies it should be pointed out that the size of the benzene dimer, despite exploiting the entire D_{6h} symmetry, severely limits the number of basis functions we are able to apply with the MP2 shielding calculations. It was not possible to go beyond the DZP basis set in the present work, and we are aware of the fact that the results are far from being converged. For example, the experimental data for the σ^{iso}(C) and σ^{iso}(H) of the isolated benzene molecule are 57.2[62] and 23.68 ppm,[63] respectively, whereas the MP2 results obtained with rather small DZP basis set are 83.1 and 24.20 ppm accordingly. Even with the TZ2P basis set the ^{13}C and ^{1}H atoms are still too shielded (the MP2/TZ2P theoretical results are σ^{iso}(C) = 65.9 ppm and σ^{iso}(H) = 23.93 ppm). In agreement with the case of the ^{15}N and ^{1}H SOS-DFPT calculations for the formamide dimer, the IGLO-III principal values of the ^{13}C and ^{1}H chemical shielding tensors and the corresponding σ^{iso}(C) and σ^{iso}(H) data for the benzene dimer are converged with respect to their JMN2 counterparts. Namely, the |IGLO-III−JMN2| differences in the computed σ_{ii}(C), σ_{ii}(H), σ^{iso}(C), and σ^{iso}(H) do not exceed 0.39, 0.23, 0.20, and 0.22 ppm, respectively. Thus, as was demonstrated earlier for the adenine−thymine base pair of nucleic acids,[48] the IGLO-III basis set can be considered saturated for the description of the chemical shielding in the SOS-DFPT-IGLO framework.

Table 3 collects the σ^{iso}(C) and CSA_a(C) values computed with the DZP basis set at the same intermonomer separations

TABLE 2: Amidic ^{1}H Isotropic Chemical Shielding (ppm) and Chemical Shielding Anisotropy (in Parentheses, ppm) at Different Vertical Separations between Formamide Monomers (*r*, Å) as Predicted by Various Approaches[a]

	DZP			DZP+			TZ2P			
r	MP2	HF	B3LYP	MP2	HF	B3LYP	MP2	HF	B3LYP	SOS-DFPT
3.0	24.15	24.17	23.68	23.86	24.02	23.40	23.62	23.97	23.32	22.94
	(4.61)	(3.06)	(3.57)	(4.25)	(2.86)	(3.19)	(4.08)	(2.94)	(3.16)	(4.06)
3.2	24.16	24.18	23.70	23.87	24.02	23.41	23.64	23.98	23.34	22.95
	(4.75)	(3.14)	(3.71)	(4.38)	(4.38)	(3.31)	(4.23)	(3.02)	(3.31)	(4.23)
3.4	24.17	24.18	23.72	23.87	24.02	23.41	23.65	23.98	23.35	22.96
	(4.86)	(3.20)	(3.81)	(4.49)	(2.98)	(3.42)	(4.35)	(3.09)	(3.43)	(4.37)
3.6	24.18	24.19	23.73	23.87	24.02	23.41	23.65	23.99	23.36	23.30
	(4.94)	(3.27)	(3.89)	(4.59)	(3.05)	(3.51)	(4.45)	(3.16)	(3.53)	(4.48)
3.8	24.19	24.19	23.73	23.87	24.02	23.41	23.66	23.99	23.37	22.98
	(5.01)	(3.34)	(3.95)	(4.67)	(3.12)	(3.59)	(4.54)	(3.23)	(3.61)	(4.58)
4.2	24.20	24.19	23.74	23.87	24.01	23.41	23.67	23.99	23.37	22.99
	(5.14)	(3.46)	(4.07)	(4.82)	(3.25)	(3.73)	(4.69)	(3.37)	(3.77)	(4.70)
4.6	24.20	24.19	23.75	23.87	24.01	23.40	23.67	23.99	23.38	22.99
	(5.24)	(3.58)	(4.16)	(4.97)	(3.38)	(3.85)	(4.81)	(3.49)	(3.89)	(4.80)
5.0	24.20	24.19	23.74	23.86	24.00	23.39	23.67	23.99	23.38	22.99
	(5.32)	(3.67)	(4.24)	(5.05)	(3.49)	(3.95)	(4.92)	(3.60)	(3.99)	(4.89)

[a] See the text for the description of respective computational methods.

TABLE 3: ^{13}C Isotropic Chemical Shielding (ppm) and Chemical Shielding Anisotropy (in Parentheses, ppm) at Different Vertical Separations between Benzene Monomers (*r*, Å) as Predicted by the GIAO-Based Approaches Employing the DZP Basis Set[a]

r	MP2	HF	B3LYP	*r*	MP2	HF	B3LYP
3.0	75.5	57.5	54.1	3.8	82.2	65.7	61.7
	(196.0)	(228.5)	(207.2)		(186.4)	(216.2)	(196.2)
3.2	78.3	61.1	57.4	4.2	83.1	66.7	62.8
	(191.9)	(223.2)	(202.5)		(184.9)	(214.4)	(194.6)
3.4	80.2	63.3	59.4	4.6	83.4	67.0	63.2
	(189.3)	(219.8)	(199.5)		(184.0)	(213.5)	(193.7)
3.6	81.4	64.8	60.8	5.0	83.5	67.0	63.2
	(187.5)	(217.6)	(197.6)		(183.5)	(213.0)	(193.2)

[a] See the text for the description of respective computational methods.

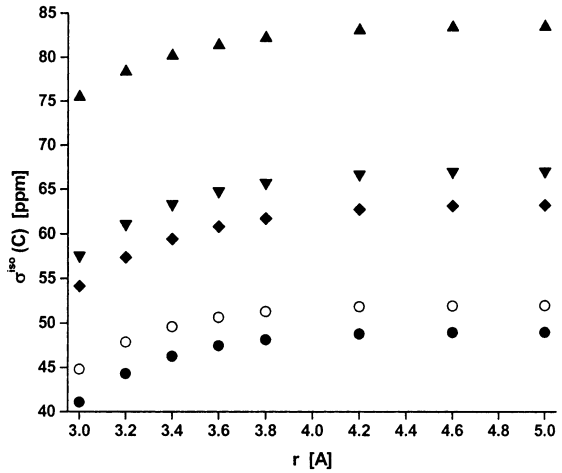

Figure 6. Plot of the ^{13}C isotropic chemical shielding in the benzene dimer σ^{iso}(C) computed at different vertical separations between monomers *r* by the MP2-GIAO/DZP (up triangles), HF-GIAO/DZP (down triangles), B3LYP-GIAO/DZP (solid circles), HF-GIAO/TZ2P (diamonds), and SOS-DFPT/IGLO−III (open circles) methods. See the text for details.

as the chemical shielding data obtained for the formamide dimer. The absolute isotropic shielding of ^{13}C nuclei is predicted to decrease significantly upon diminishing the distance between monomers. This holds for the HF/TZ2P, B3LYP/TZ2P and SOS-DFPT data as well (cf. Figure 6).

Interestingly, an almost-perfect fit (data not given) of this decrease can be obtained by using the three-parameter form given by eq 6, which we have successfully applied to describe the relationship between the σ^{iso}(N) and the vertical separation *r* in the case of nonaromatic stacking (see the Formamide Dimer section). This model works also for, for example, the ^{15}N and ^{13}C isotropic chemical shielding in formamidine and pyrimidine homodimers (cf. Supporting Information Tables 20S−31S) and in stacked nucleobases,[24] which is an indication of a more general trend. Further, the MP2/DZP results for the σ^{iso}(C) are higher than their HF/DZP counterparts, whereas the |MP2 − HF| differences remain approximately the same within the investigated range of *r* values. Namely, the |MP2 − HF| data lie between 16.40 and 17.95 ppm with the mean value of 16.79 ppm and the standard deviation of only 0.194 ppm. Thus, the effect of correlation has a negligible influence on the differences, which are brought about by the stacking of two benzene molecules, between σ^{iso}(C)'s at different intermonomer distances. The relative unimportance of a contribution to the chemical shielding due to the effects of electron correlation has been observed in a number of other systems.[24] For example, the |MP2 − HF| data obtained for the formamidine dimer employing the DZP+ basis set lie between 25.10 and 25.18 ppm (mean value 25.15 ppm, standard deviation 0.033 ppm) in the case of the σ^{iso}(C) (see Table 20S) and between 9.73 and 10.12 ppm (mean value 10.02 ppm, standard deviation 0.136 ppm) for the isotropic amino ^{15}N chemical shielding (Table 23S).

Figure 7 shows the CSA_a(C) data as calculated by several methods. In agreement with results obtained for isolated benzene at the Hartree−Fock level using ample basis sets,[64] an extension of the basis set causes a pronounced deshielding effect on σ_{11} and σ_{22} principal elements thus leading to an increase of the ^{13}C chemical shielding anisotropy. In accord with a high-level treatment of the monomer,[63] correlation effects cause strong (20−30 ppm) shielding of σ_{11} and σ_{22} and remain σ_{33} practically unaffected (cf. Tables 13S−18S). Nonetheless, all methods and basis sets predict an exponential decrease of the CSA_a(C) with the monomer separation (Figure 7).

Table 4 contains the values of the isotropic chemical shielding and CSA_a of the ^{1}H nuclei in the vertically displaced benzene dimers computed by the HF, MP2, and B3LYP methods using the DZP basis set. It can be of some interest to compare the changes in the σ^{iso}(H) with the distance between benzene monomers obtained by an explicit quantum chemical calculation to those resulting from a simple and popular model first proposed by McConnell.[49] In the latter approach, one of the

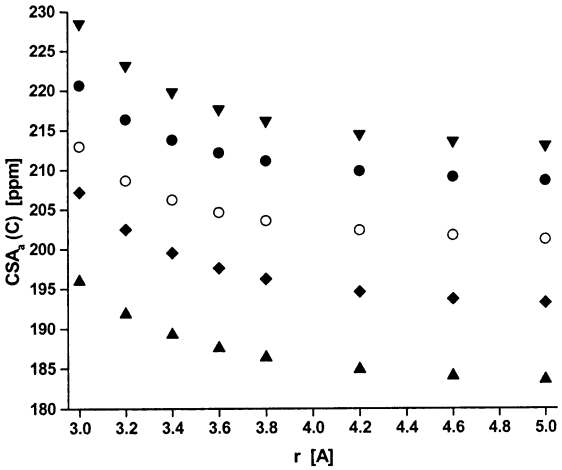

Figure 7. Plot of the ^{13}C chemical shielding anisotropy in the benzene dimer σ^{iso}(C) computed at different vertical separations between monomers *r* by the MP2-GIAO/DZP (up triangles), HF-GIAO/DZP (down triangles), B3LYP-GIAO/DZP (solid circles), HF-GIAO/TZ2P (diamonds), and SOS-DFPT/IGLO−III (open circles) methods. See the text for details.

TABLE 4: ^{1}H Isotropic Chemical Shielding (ppm) and Chemical Shielding Anisotropy (in Parentheses, ppm) at Different Vertical Separations between Benzene Monomers (*r*, Å) as Predicted by the GIAO-Based Approaches Employing the DZP Basis Set[a]

r	MP2	HF	B3LYP	*r*	MP2	HF	B3LYP
3.0	24.61	24.68	24.50	3.8	24.66	24.76	24.57
	(5.11)	(6.09)	(6.20)		(3.81)	(4.16)	(3.92)
3.2	24.69	24.78	24.59	4.2	24.62	24.69	24.50
	(4.37)	(5.07)	(5.08)		(3.80)	(4.06)	(3.73)
3.4	24.71	24.80	24.61	4.6	24.55	24.62	24.44
	(4.05)	(4.57)	(4.48)		(3.87)	(4.11)	(3.72)
3.6	24.70	24.79	24.60	5.0	24.50	24.57	24.39
	(3.89)	(4.31)	(4.14)		(4.01)	(4.23)	(3.80)

[a] See the text for the description of respective computational methods.

benzene molecules is treated as the "remote chemical group" which modifies the isotropic chemical shift of a proton of the second benzene by an amount $\Delta\delta$ given by eq 3 (see the Methods section). The B3LYP−CSGT/TZ2P approach adopted here gives the principal elements of the magnetizability tensor of benzene in a good agreement with experiment. Namely, in the units of ppm Å^3/molecule, $\chi_{11} = -162.7$, $\chi_{22} = \chi_{33} = -55.9$, whereas the experimental data are $\chi_{11} = -157.1$, $\chi_{22} = \chi_{33} = -57.9$.[64] Hence, the DFT value of the anisotropy of the magnetizability tensor of benzene (−106.8) is close to the experimental $\chi^{aniso} = -99.2$ ppm Å^3/molecule and has been entered into McConnell eq 3 (see the Methods section). The B3LYP−CSGT/TZ2P shielding data are given in Supporting Information Table 19S. The values of the isotropic shielding calculated at the separations from 3.0 up to 15.0 Å, relative to the σ^{iso}(H) in the isolated benzene, are shown of Figure 8 together with the $\Delta\delta$ values as predicted by McConnell equation. Because of the well-known "close-contact" effects,[16] the McConnell theory fails completely below 3.6 Å. However, at larger distances, this approximation is quite successful. An agreement between the DFT supermolecular results and McConnell equation can be further improved by finding an "effective susceptibility anisotropy", *K*. This is obtained by writing down eq 4 (cf. the Methods section) to contain *K* as a coefficient

$$\Delta\delta(r;K) = K\frac{2r^2 - d^2}{3(d^2 + r^2)^{5/2}} \qquad (7)$$

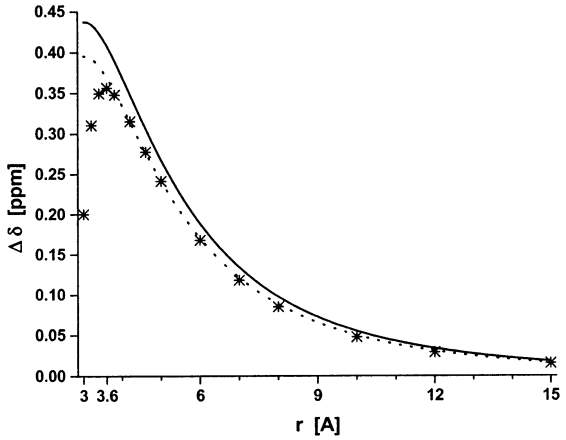

Figure 8. Contributions to the isotropic chemical shift of proton in benzene $\Delta\delta$ due to the presence of a stacking benzene molecule at the vertical separation *r* as predicted by the B3LYP−CSGT/TZ2P method (stars), and by two forms of a McConnell-type model, i.e., eqs 3 and 7 described in the text (solid and dotted line accordingly).

and performing the least-squares fit between the B3LYP−CSGT/TZ2P data from the interval ⟨3.60;15.0⟩ Å and the values computed from eq 7. The resulting $K = -89.7$ is still fairly close to the values of susceptibility anisotropy discussed above and leads to an almost-perfect agreement between the McConnell model and the quantum chemical results considered (see Figure 8). This straightforward procedure can be employed to relate the McConnell model to shielding results obtained by the remaining approaches (data not given).

Conclusion

Current quantum mechanical methods of ab initio chemical shielding calculations allow one to explore in a systematic way the variation in the chemical shielding parameters due to a variety of intermolecular interactions. Here several such approaches have been combined with basis sets of different size and quality to monitor the isotropic chemical shielding and the chemical shielding anisotropy of the ^{15}N, ^{1}H, and ^{13}C nuclei at different vertical-stacking distances in the formamide and benzene dimers. Although the computational strategies employed differ in the way they treat the effects of electron correlation and hence their ability to account for the energetics of stacking varies significantly, the qualitative characteristics of the stacking-induced variation in the isotropic chemical shielding and the chemical shielding anisotropy remain unchanged. In particular, the HF and DFT values of the σ^{iso}(N) in the formamide homodimers, and of the σ^{iso}(C) in the benzene homodimers, are uniformly deshielded with respect to the MP2 data. Namely, the |MP2 − HF| differences obtained for the σ^{iso}(N) employing the TZ2P basis set lie between 7.88 and 8.28 ppm (mean value 8.18 ppm, standard deviation 0.138 ppm); in the case of the σ^{iso}(C) studied using the DZP basis set, they lie between 16.40 and 17.95 ppm (mean value of 16.79 ppm, standard deviation 0.194 ppm). As a result of this relative unimportance of the level of treatment of electron correlation contributions to the chemical shielding tensors, an application of the computationally cheap, DFT-based methods (the SOS-DFPT-IGLO strategy in particular) to the modeling chemical shielding parameters of stacked complexes is justified.

Of special interest is the finding that both the ^{15}N (in FD) and ^{13}C (in BD) isotropic chemical shielding is predicted to increase exponentially with the intermonomer separation according to a simple parametrization given by eq 6. Such

relationships, which have been shown here to hold also in the formamidine and pyrimidine homodimers, could be developed into a useful probe of the structure of complex systems.[24] Moreover, the contribution of stacking to the ^{1}H isotropic chemical shifts in the benzene dimer has been successfully modeled using a modified McConnell model[49] at the intermonomer separations higher than 3.60 Å. An analogous approach can be employed in an estimation of the ring-current effects on the proton chemical shifts in nucleic acids.[24]

Acknowledgment. I thank Dr. Nikolai R. Skrynnikov for a discussion of and an early access to his manuscript (ref 15). This research has been supported by the Grant Agency of the Academy of Sciences of the Czech Republic, Grants AVOZ4050913 and KJB4050311. Time allocation in the Czech Academic Supercomputer Centre and in the Mississippi Center for Supercomputing Research is gratefully acknowledged.

Supporting Information Available: An analysis of the HF, B3LYP, and MP2 interaction energies for the formamide and benzene homodimers (Tables 1S−4S). Principal components of the respective ^{15}N, ^{1}H, and ^{13}C shielding tensors as predicted by different methods for the formamide and benzene homodimers (Tables 5S−19S), and for the formamidine and pyrimidine homodimers (Tables 20S−31S). This material is available free of charge via the Internet at http://pubs.acs.org.

References and Notes

(1) Brutschy, B.; Hobza P. *Chem. Rev.* **2000**, *100*, 3861−3862.
(2) Chelli, R.; Gervasio, F. L.; Procacci, P.; Schettino, V. *J. Am. Chem. Soc.* **2002**, *124*, 6133−6143.
(3) Saenger, W. *Principles of Nucleic Acid Structure*; Springer-Verlag: New York, 1984.
(4) Chow, C. S.; Bogdan, F. M. *Chem. Rev.* **1997**, *97*, 1489−1513.
(5) Řeha, D.; Kabeláč, M.; Ryjáček, F.; Šponer, J.; Šponer, J. E.; Elstner, M.; Suhai, S.; Hobza, P. *J. Am. Chem. Soc.* **2002**, *124*, 3366−3766.
(6) Tsuzuki, S.; Honda, K.; Uchimaru, T.; Mikami, M.; Tanabe, K. *J. Am. Chem. Soc.* **2002**, *124*, 104−112.
(7) Hobza, P.; Šponer, J. *Chem. Rev.* **1999**, *99*, 3247−3276.
(8) Leininger, M. L.; Nielsen, I. M. B.; Colvin, M. E.; Janssen, C. L. *J. Phys. Chem. A* **2002**, *106*, 3850−3854.
(9) Guckian, K. M.; Schweitzer, B. A.; Ren, R. X.-F.; Sheils, C. J.; Tahmassebi, D. C.; Kool, E. T. *J. Am. Chem. Soc.* **2000**, *122*, 2213−2222.
(10) Steullet, V.; Dixon, D. W. *J. Chem. Soc., Perkin Trans. 2* **1999**, *7*, 1547−1558.
(11) Burini, A.; Fackler, J. P., Jr.; Galassi, R.; Macchioni, A.; Omary, M. A.; Rawashdeh-Omary, M. A.; Pietroni, B. R.; Sabatini, S.; Zuccaccia, C. *J. Am. Chem. Soc.* **2002**, *124*, 4570−4571.
(12) Zhang, X.; Gaffney, B. L.; Jones, R. A. *J. Am. Chem. Soc.* **1998**, *120*, 615−618.
(13) Lazzeretti, P. *Prog. NMR Spectrosc.* **2000**, *36*, 1−88.
(14) Brown, S. P.; Schnell, T.; Brand, J. D.; M_llen, K.; Spiess, H. W. *J. Am. Chem. Soc.* **1999**, *121*, 6712−6718.
(15) Boyd, J.; Skrynnikov, N. R. *J. Am. Chem. Soc.* **2002**, *124*, 1832−1833.
(16) Sitkoff, D.; Case D. A. *Prog. NMR Spectrosc.* **1998**, *32*, 165−190.
(17) Helgaker, T.; Jaszuński, M.; Ruud, K. *Chem. Rev.* **1999**, *99*, 293−352.
(18) Cui, Q.; Karplus, M. *J. Phys. Chem. B* **2000**, *104*, 3721−3743.
(19) Xu, X. P.; Au−Yeung, S. C. F. *J. Phys. Chem. B* **2000**, *104*, 5641−5650.
(20) Parr, R. G.; Yang, W. *Density-Functional Theory of Atoms and Molecules*; Oxford University Press: Oxford, 1989.
(21) Ochsenfeld, C.; Brown, S. P.; Schnell, I.; Gauss, J.; Spiess, H. W. *J. Am. Chem. Soc.* **2001**, *123*, 2597−2606.
(22) Šponer, J.; Hobza, P. *Chem. Phys. Lett.* **1997**, *267*, 263−270.
(23) Case, D. A. *J. Biomol. NMR* **1995**, *6*, 341−346.
(24) Czernek, J. In progress.
(25) Dahl, T. *Acta Chem. Scand.* **1994**, *48*, 95−106.
(26) Dunning, T. H., Jr. *J. Chem. Phys.* **1970**, *53*, 2823.
(27) Dunning, T. H., Jr.; Hay, P. J. In *Methods of Electronic Structure Theory*; Schaefer, H. F., III., Ed.; Plenum Press: New York, 1977; Vol. 3.
(28) Basis sets were obtained from the Extensible Computational Chemistry Environment Basis Set Database, Version 1/13/03, as developed and distributed by the Molecular Science Computing Facility, Environmental and Molecular Sciences Laboratory which is part of the Pacific Northwest Laboratory, P.O. Box 999, Richland, WA 99352, USA, and funded by the U.S. Department of Energy. The Pacific Northwest Laboratory is a multiprogram laboratory operated by Battelle Memorial Institue for the U.S. Department of Energy under contract DE-AC06-76RLO 1830. Contact David Feller or Karen Schuchardt for further information.
(29) Šponer, J.; Berger, I.; Špačková, N.; Leszczynski, J.; Hobza, P. *J. Biomol. Struct. Dyn.* **2000**, *S2* (11th Conversation Special Issue), 383−407.
(30) Vargas, R.; Garza, J.; Dixon, D. A.; Hay, B. P. *J. Am. Chem. Soc.* **2000**, *122*, 4750−4755.
(31) Schäfer, A.; Horn, H.; Ahlrichs, R. *J. Chem. Phys.* **1992**, *97*, 2571−2577.
(32) Kutzelnigg, W.; Fleischer, U.; Schindler, M. *NMR Basic Principles and Progress*; Springer-Verlag: Berlin, 1990; Vol. 23, p 165.
(33) Malkin, V. G.; Malkina, O. L.; Eriksson, L. A.; Salahub, D. R. In *Theoretical and Computational Chemistry*; Seminario, J. M., Politzer, P., Eds.; Elsevier: Amsterdam, 1995; Vol. 2, p 273.
(34) Gauss, J. *Chem. Phys. Lett.* **1992**, *191*, 614−620.
(35) Ditchfield, R. *Mol. Phys.* **1974**, *27*, 789−805.
(36) Wolinski, K.; Hinton, J. F.; Pulay, P. *J. Am. Chem. Soc.* **1990**, *112*, 8251.
(37) Frisch, M. J.; Trucks, G. W.; Schlegel, H. B.; Scuseria, G. E.; Robb, M. A.; Cheeseman, J. R.; Zakrzewski, V. G.; Montgomery, J. A., Jr.; Stratmann, R. E.; Burant, J. C.; Dapprich, S.; Millam, J. M.; Daniels, A. D.; Kudin, K. N.; Strain, M. C.; Farkas, O.; Tomasi, J.; Barone, V.; Cossi, M.; Cammi, R.; Mennucci, B.; Pomelli, C.; Adamo, C.; Clifford, S.; Ochterski, J.; Petersson, G. A.; Ayala, P. Y.; Cui, Q.; Morokuma, K.; Malick, D. K.; Rabuck, A. D.; Raghavachari, K.; Foresman, J. B.; Cioslowski, J.; Ortiz, J. V.; Stefanov, B. B.; Liu, G.; Liashenko, A.; Piskorz, P.; Komaromi, I.; Gomperts, R.; Martin, R. L.; Fox, D. J.; Keith, T.; Al-Laham, M. A.; Peng, C. Y.; Nanayakkara, A.; Gonzalez, C.; Challacombe, M.; Gill, P. M. W.; Johnson, B. G.; Chen, W.; Wong, M. W.; Andres, J. L.; Head-Gordon, M.; Replogle, E. S.; Pople, J. A. *Gaussian 98*, revision A.7; Gaussian, Inc.: Pittsburgh, PA, 1998.
(38) Becke, A. D. *J. Chem. Phys.* **1993**, *98*, 5648−5652.
(39) Lee, C.; Yang, W.; Parr, R. *Phys. Rev. B* **1998**, *37*, 785−789.
(40) Cheeseman, J. R.; Trucks, G. W.; Keith, T. A.; Frisch, M. J. *J. Chem. Phys.* **1996**, *104*, 5497−5509.
(41) Salahub, D. R.; Fournier, R.; Mlynarski, P.; Papai, A.; St-Amant, A.; Uskio, J. In *Density Functional Methods in Chemistry*; Labanowski, J., Andzelm, J. W., Eds.; Springer: New York, 1991; p 77.
(42) Malkin, V. G.; Malkina, O. L.; Salahub, D. R. *MASTER−CS Program*; Universite de Montreal: Montreal, 1994.
(43) Perdew, J. P.; Wang, Y. *Phys. Rev. B* **1992**, *45*, 13244−13249.
(44) Perdew, J. P.; Chevary, J. A.; Vosko, S. H.; Jackson, K. A.; Pederson, M. R.; Singh, D. J.; Fiolhais, C. *Phys. Rev. B* **1992**, *46*, 6671−6687.
(45) Malkin, V. G.; Malkina, O. L.; Casida, M. E.; Salahub, D. R. *J. Am. Chem. Soc.* **1994**, *116*, 5898−5908.
(46) Boys, S. F. In *Quantum Theory of Atoms, Molecules and the Solid State*; Löwdin, P.-O., Ed.; Academic Press: New York, 1996; p 263.
(47) Czernek, J.; Fiala, R.; Sklená, V. *J. Magn. Reson.* **2000**, *145*, 142−146.
(48) Czernek, J. *J. Phys. Chem. A* **2001**, *105*, 1357−1365.
(49) McConnell, H. M. *J. Chem. Phys.* **1957**, *27*, 226−229.
(50) Keith, T. A.; Bader, R. W. F. *Chem. Phys. Lett.* **1992**, *194*, 1−8.
(51) Keith, T. A.; Bader, R. W. F. *J. Chem. Phys.* **1993**, *99*, 3669−3682.
(52) Bader, R. W. F.; Keith, T. A. *J. Chem. Phys.* **1993**, *99*, 3683−3693.
(53) Boys, S. F.; Bernardi, F. *Mol. Phys.* **1970**, *19*, 553−563.
(54) See: Sinnokrot, M. O.; Valeev, E. F.; Sherrill, C. D. *J. Am. Chem. Soc.* **2002**, *124*, 10887−10893 and references therein.
(55) Hobza, P.; Šponer, J. *J. Mol. Struct. (THEOCHEM)* **1996**, *388*, 115−120.
(56) See: van Mourik, T.; Gdanitz, R. J. *J. Chem. Phys.* **2002**, *116*, 9620−9623 and references therein.
(57) Wilson, P. J.; Tozer, D. J. *J. Chem. Phys.* **2002**, *116*, 10139−10147.
(58) Barich, D. H.; Nicholas, J. B.; Haw, J. F. *J. Phys. Chem. A* **2001**, *105*, 4708−4715.
(59) Chesnut, D. B. *Chem. Phys. Lett.* **1995**, *246*, 235−238.
(60) Czernek, J.; Sklená, V. *J. Phys. Chem. A* **1999**, *103*, 4089−4093.
(61) Sharma, Y.; Kwon, O. Y.; Brooks, B.; Tjandra, N. *J. Am. Chem. Soc.* **2002**, *124*, 327−335.
(62) Jameson, A. K.; Jameson, C. J. *Chem. Phys. Lett.* **1987**, *134*, 461−466.
(63) Lazzeretti, P.; Zanasi, R. *J. Chem. Phys.* **1981**, *75*, 5019−5027.
(64) Lazzeretti, P.; Malagoli, M.; Zanasi, R. *J. Mol. Struct. (THEOCHEM)* **1991**, *234*, 127−145.
(65) Bouman, T. D.; Hansen, Aa. E. *Chem. Phys. Lett.* **1992**, *197*, 59−66.